https://doi.org/10.1016/j.compchemeng.2021.107552

Improved design of heat-pump extractive distillation based on the process optimization and multi-criteria sustainability analysis

Tao Shi[1], Yue Liu[1], Haoshui Yu[2], Ao Yang[1,3], Shirui Sun[3], Weifeng Shen[3], Carman K.M. Lee[1], Jingzheng Ren[1]*

[1]Department of Industrial and Systems Engineering, The Hong Kong Polytechnic University, Hong Kong SAR, P. R. China

[2]Department of Chemistry and Bioscience, Aalborg University, Niels Bohrs Vej 8A, Esbjerg 6700, Denmark

[3]School of Chemistry and Chemical Engineering, Chongqing University, Chongqing 400044, P. R. China

Corresponding Author: *E-mail: jzhren@polyu.edu.hk

Abstract

In order to achieve the sustainable separation design of azeotropic mixtures, this study proposed a systematic framework for distillation process optimization and intensification based on a composite sustainability index. Binary minimum azeotropic mixture ethanol-ethyl propionate was studied as an illustrative example. Specifically, three extractive distillation configurations were firstly applied on the separation and the sustainability of distillation processes were evaluated comprehensively. The composite sustainability index was constructed with the indicators of the economic, environmental, technical and social dimensions, and fuzzy weighting method was used to determine the weight of each indicator. Then, the process can be optimized with the objective of the composite sustainability index by the mesh adaptive direct search algorithm. After that, the heat-pump is further implemented to make full use of the latent heat of vapor stream in the distillation system . The T-H diagram of two upgraded processes clearly demonstrates the heat recovery while considering the specified minimum heat-transfer temperature difference.

Keywords: Extractive distillation, Heat-pump technique, Process optimization, Sustainability analysis, Composite sustainability index

1. Introduction

From the perspective of technology maturity, special distillation such as extractive distillation (ED) [1, 2], pressure-swing distillation [3, 4], heterogenous azeotropic distillation [5, 6], and reactive distillation [7, 8] are widely used in practical chemical industry for the separation of azeotropic mixtures. However, in special distillation one of the challenges is how to efficiently use the energy and design sustainable processes because of its energy-intensive feature [9]. Accordingly, some process intensification methods like heat-integration operation or heat-pump assisted distillation were introduced to make improvements [10, 11]. Of note is that the heat-integrated distillation configuration may pose some dynamic difficulties associated with control design because of its less feasibility and fewer degrees of freedom, although it has the potential of large energy savings [12, 13]. In terms of the steady state design, Gu *et al.* [14] achieved the energy-saving heat-integration design by adjusting the pressure of an extractive distillation column. Wang *et al.* [15] improved the economic performance and energy efficiency of triple-column pressure-swing distillation by upgrading the low-level heat source of the vapor stream and using heat-pump technology. Their results have proved the economic superiority of incorporating heat-pump and heat-integration schemes into distillation design for the separation of various azeotropic mixtures. Nevertheless, their assessment work only focused on the economic cost aspect. Other sustainability aspects such as environmental, social and safety aspects should also be considered in the process design [16].

Incorporating sustainability metrics in the process design, evaluation and optimization can help decision-makers master the associated process design problem more accurately and comprehensively [17-19]. There are 17 sustainable development goals which can be mainly categorized into three aspects namely environment, economy and society [20]. Few works in distillation process design focused on sustainable-oriented optimization by considering all sustainability aspects simultaneously. Some studies focused on the minimization of economic objectives [21, 22] while some others also included environmental objectives [23, 24]. It is more usual that some sustainability indicators were used in the methods for optimizing a process and the remaining indicators were consequentially calculated and compared [25]. Therefore, it is found that evaluation objectives in the optimization are usually equal or less than three (economy, environment and society are the three pillars of sustainability), and it means that the previous multi-criteria sustainability optimization has one significant weakness – it is difficult or even impossible to incorporate more sustainability objectives. The main reason for not considering more sustainability sub-indicators in multi-objective optimization is the huge computational burden growing exponentially when the number of objectives increase. To solve the problem, Guillén-Gosálbez [26] removed some redundant criteria from multi-objective optimization models to simplify the computation and the analysis of their Pareto solutions. In order to fill this research gap differently, a composite sustainability index (CSI) which incorporates the economic, environmental, social and technical performances simultaneously was established in this study. CSI is a measure of the holistic sustainability of a distillation process. By converting the multiple sustainability indicators into a composite optimization objective, identification of the desirable result becomes straightforward, and a stable optimization result can be obtained because there is no need to make further discussion from the Pareto front. In addition, the computational burden growing substantially with the number of objectives can be further decreased. Although the concept of CSI has been used in a brewery and sludge-to energy prioritization [27, 28], few works applied this concept on the distillation design to solve some specified multi-criteria sustainability evaluation problems.

Sustainability-oriented optimization should be considered in the process design because the stakeholders want the optimal results by achieving some specified goals such as the relatively lower economic cost, maximized profit and small environmental impacts. The sequential iteration optimization procedure was applied to solve the optimization problem of complex distillation processes in the previous study [29], but this procedure could not simultaneously evaluate the influence of all decision variables. Also, the sequential quadratic programming (SQP) optimization method that is available in Aspen Plus was hard to make the simulation converge when relatively more discrete variables exist. Nowadays, stochastic optimization algorithms such as mesh adaptive direct search algorithm (MADS) [30], genetic algorithm [31], simulated annealing algorithm [32], and particle swarm algorithm [33] have been increasingly popular in chemical process systems for solving such optimization problems. Rangaiah *et al.* [34] have given a comprehensive introduction about the process optimization problem which is conducive to learning. MADS algorithm could be readily called in Matlab tool to solve practical simulation problems with the help of a package NOMAD-Nonlinear Optimization by Mesh Adaptive Direct search [35]. In addition, MADS can efficiently explore different variable spaces to search for better solutions for a large spectrum of optimization problems [36]. Therefore, MADS algorithm was finally used in the proposed framework and detailed information about this has been presented in the methodology section.

In this study, we have proposed a systematic framework to achieve the sustainable distillation process design considering the optimization of multiple sustainability-oriented objectives. Those measurable sustainability sub-indicators are firstly aggregated into a CSI through fuzzy weighting and linear aggregation approaches. Compared with a multi-objective optimization problem, the optimization of a single objective CSI can be achieved with a less computational burden. To validate the proposed procedure, a case study of separating the binary azeotropic mixture ethanol (EtOH) and ethyl propionate (EtPA) was investigated. Of note is that the process-scale separation by extractive distillation has not been comparatively studied and evaluated systematically before [37, 38]. Specifically, three ED alternatives for the separation are obtained and optimized, which involves a short-cut selection of the suitable entrainer, the construction of CSI and process optimization by MADS. The obtained promising ED scheme is further improved through heat-pump technique and heat integration design to make full use of the latent heat of vapor stream in the distillation system itself. Multi-criteria sustainability analysis was finally carried out to compare the performance in terms of economic, environmental, social and technical sustainability in an integrated manner.

2. Methodology

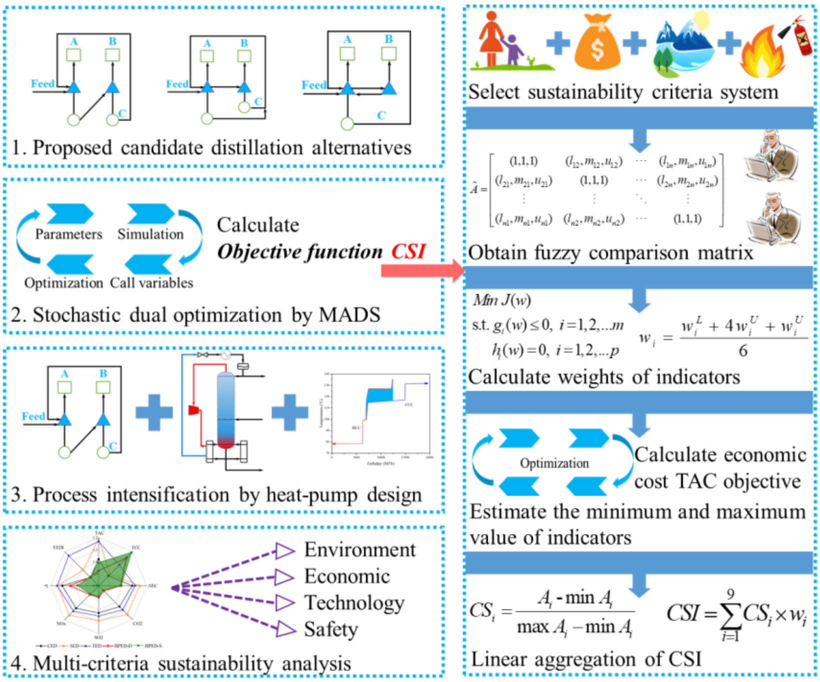

Fig. 1. The proposed framework for the process design and multi-criteria sustainability analysis in distillation process design

In this work, a systematic module approach for the process optimization and multi-criteria sustainability analysis of the distillation processes has been proposed (see **Fig. 1**). Firstly, different distillation schemes were proposed and simulated. Subsequently, those distillation configurations were optimized with the constructed CSI objective. Then, based on process intensification, one of the sustainable ED configurations was improved by applying the heat-pump technology. Finally, a multi-criteria sustainability evaluation and comparison was presented in detail. The case study for separating EtOH-EtPA mixture has been investigated based on the proposed framework. The construction of CSI has five steps. The first step is to select sustainability criteria system and different indicators applied in the study. Then the triangular fuzzy comparison matrix is obtained based on transformation rules of linguistic variables of decision-makers. After that, a typical nonlinear optimization model can be solved to calculate the weights of each indicator. And the optimization of a single economic objective identifies the minimum and maximum value with respect to other indicators in the normalization step. Eventually, the CSI incorporating the economic, environmental, technical and safety indicators can be determined by the linear aggregation method.

2.1 Composite sustainability index

CSI as an aggregation of the economic, environmental, safety and technical performances can be readily used to represent the integrated sustainability performance of a process. Accordingly, a single-objective optimization model maximizing the CSI can be developed. It can trade off among multiple sustainability-oriented objectives . In order to construct the composite sustainability index, a criteria system should be first built up which includes relevant indicators in different pillars of sustainability. The indicators for sustainability assessment and the methods for the calculation of these indicators have been presented in Section 2.4. It is a prerequisite to determine the weights of these indicators because different indicators play different roles in sustainable development and the stakeholders may also have different preferences on these indicators. There are various basic weighting methods such as the best-worst method (BWM) [39], analytical hierarchy process (AHP) [40], and the multi-attribute utility theory (MAUT) [41]. In this study, AHP method which has been widely used in decision-making process was adopted. It is based on the theory for relative measurement *via* step-to-step comparison and calculation [42]. Traditionally, eigenvector method was applied to derive the weight vector in an AHP analysis. And it was shown in the following equation [43].

$$A\vec{w} = \begin{pmatrix} w_1/w_1 & w_1/w_2 & \cdots & w_1/w_n \\ w_2/w_1 & w_2/w_2 & \cdots & w_2/w_n \\ \vdots & \vdots & \ddots & \vdots \\ w_n/w_1 & w_n/w_2 & \cdots & w_n/w_n \end{pmatrix} \begin{pmatrix} w_1 \\ \vdots \\ w_n \end{pmatrix} = \lambda \begin{pmatrix} w_1 \\ \vdots \\ w_n \end{pmatrix} \tag{1}$$

However, the true weights ratios (i.e., w_i/w_j) are difficult to know and the comparison judgement is finished in an uncertain environment. Assume the estimated weights ratio is a_{ij} and only in the perfect rationality, the relation $a_{ij} = w_i / w_j \ \forall i, j$ is right. Taking the difference between a_{ij} and w_i/w_j into account, therefore, it is fair to consider $\sum_{i=1}^{n}\sum_{j=1}^{n}\left(a_{ij} - w_i / w_j\right)^2$ as the distance between subjective comparison matrix $\left(a_{ij}\right)_{n\times n}$ and the true weight ratio matrix $\left(w_i/w_j\right)_{n\times n}$ associated with the weight vector $\vec{w}$. Further, the natural logarithmic least square is introduced to the mathematical problem [44] and it can be expressed by the following equation.

$$\begin{aligned} &\underset{(w_1,w_2\ldots w_n)}{minimize} \sum_{i=1}^{n}\sum_{j=1}^{n}\left(lna_{ij} - ln\left(\frac{w_i}{w_j}\right)\right)^2 \\ &subject\ to \sum_{i=1}^{n} w_i = 1, w_i > 0\ \forall i \end{aligned} \tag{2}$$

As shown in **Eq. (2)**, the estimated a_{ij} is significant in the solution of weight vector $\vec{w}$. Basically, entries a_{ij} in a pairwise comparison matrix reflects linguistic preference and ambiguity which cannot be accurately described by classical set theory [45]. Therefore, fuzzy AHP with optimizing the sum of logarithmic least squares was applied based on the reference [46]. It has the advantage of deriving normalized triangular fuzzy weights for both complete and incomplete triangular fuzzy comparison matrices [47]. The weight vector $\vec{w}$ is calculated as the minimum of a constrained optimization problem. Above all, the complete construction of the CSI is demonstrated as the following procedures.

(1) Identify the criteria system $\{C_1, C_2 \cdots C_n\}$, and n is the number of pillars of sustainability or the number of indicators in each pillar.

(2) Determine the fuzzy comparison matrix between those criteria according to the transformation rules of linguistic variables and triangle fuzzy numbers (see **Table 1**).

Table 1. Transformation of linguistic terms and triangle fuzzy numbers [48]

Linguistic terms	Triangle fuzzy number
Equally importance	(1,1,1)
Weakly importance	(2/3,1,3/2)
Fairly important	(3/2,2,5/2)
Very important	(5/2,3,7/2)
Absolute important	(7/2,4,9/2)

For instance, if the decision-maker thinks that the relative importance of one indicator (C_1) comparing with another indicator (C_2) is “Very important”, then the fuzzy number (5/2,3,7/2) will be used to describe the importance comparison of C_1 to C_2. Thus, the generalized form of triangular fuzzy comparison matrix $\tilde{A}$ can be expressed by **Eq. (3)** [47].

$$\tilde{A} = \begin{array}{c} \\ C_1 \\ C_2 \\ \vdots \\ C_n \end{array} \begin{array}{c} \begin{array}{cccc} C_1 & C_2 & \cdots & C_n \end{array} \\ \begin{pmatrix} (1,1,1) & (l_{12}, m_{12}, u_{12}) & \cdots & (l_{1n}, m_{1n}, u_{1n}) \\ (l_{21}, m_{21}, u_{21}) & (1,1,1) & \cdots & (l_{2n}, m_{2n}, u_{2n}) \\ \vdots & \vdots & \ddots & \vdots \\ (l_{n1}, m_{n1}, u_{n1}) & (l_{n2}, m_{n2}, u_{n2}) & \cdots & (1,1,1) \end{pmatrix} \end{array} \tag{3}$$

where C_n represents the (n)th sustainability aspect or the specified indicator of each sustainability aspect. And $\tilde{a}_{ij} = (l_{ij}, m_{ij}, u_{ij}),\ (i, j = 1, 2 \cdots n,\ i \neq j)$ represents the relative fuzzy preference of criterion i to j, in which l_{ij}, m_{ij} and u_{ij} are lower, middle and upper values of the triangular fuzzy number $\tilde{a}_{ij}$. In addition, $\tilde{a}_{ji}$ can be calculated by the reciprocal of $\tilde{a}_{ij}$ (see **Eq. (4)**).

$$\tilde{a}_{ji} = \tilde{a}_{ji}^{-1} = (1/u_{ij}, 1/m_{ij}, 1/l_{ij}) \tag{4}$$

(3) Calculate the fuzzy weights for each criterion C_n by solving the fuzzy LLSM problem as illustrated in **Eq. (5)** [47]. It is a constrained nonlinear optimization mathematical model with linear constraints which can be solved by the optimization software LINGO.

$$\begin{gathered} Min\ J = \sum_{i=1}^{n} \sum_{j=1, j\neq i}^{n} \Big(\left(\ln w_i^L - \ln w_j^U - \ln a_{ij}^L\right)^2 + \left(\ln w_i^M - \ln w_j^M - \ln a_{ij}^M\right)^2 \\ + \left(\ln w_i^U - \ln w_j^L - \ln a_{ij}^U\right)^2 \Big) \\ s.t. \begin{cases} w_i^L + \sum\limits_{j=1, j\neq i}^{n} w_j^U \geq 1, \\ w_i^U + \sum\limits_{j=1, j\neq i}^{n} w_j^L \leq 1, \\ \sum\limits_{i=1}^{n} w_i^M = 1, & i = 1, 2 \ldots n, \\ \sum\limits_{i=1}^{n} \left(w_i^L + w_i^U\right) = 2, \\ w_i^U \geq w_i^M \geq w_i^L > 0 \end{cases} \end{gathered} \tag{5}$$

where w_i^L, w_i^M, w_i^U are the lower, middle and upper values of the normalized triangular fuzzy weights $\tilde{w}_i = (w_i^L, w_i^M, w_i^U)\ (i = 1, 2, \cdots n)$ respectively. Other values like w_j^L, w_j^M, w_j^U in the normalized triangular fuzzy weights $\tilde{w}_j$ can be expressed similarly. $a_{ij}^L, a_{ij}^M, a_{ij}^U$ are the lower, middle and upper values of the triangular fuzzy judgements $\tilde{a}_{ij}$, respectively.

(4) According to the study by Guo and Zhao [48], the final defuzzied weight of each criterion is determined based on **Eq. (6)**. Since there are two levels of indicators, the weight of sustainability aspects and that of indicators in each sustainability aspect must be calculated via **Eq.(5)**. The global weight of criterion *j* equals to the local weight for each aspect multiply the local weight for each criterion with respect to the sustainability aspect (see **Eq. (7)**). Then normalization is needed to get the final global weight of each criterion as given by **Eq. (8)**.

$$w_i = \frac{w_i^L + 4w_i^M + w_i^U}{6} \tag{6}$$

$$w_j^{'} = w_{AS_i} \times w_{ij} \tag{7}$$

$$w_j = \frac{w_j^{'}}{\sum_j^n w_j^{'}} \tag{8}$$

where w_i^L, w_i^M, w_i^U are the lower, middle and upper values of the normalized triangular fuzzy weight $\tilde{w}_i$. The local weight for each aspect is represented by w_{AS_i}. w_{ij} stands for the local weight for each indicator with respect to sustainability aspects. In addition, w_j is the final global weight of each specified criterion *j*.

(5) Aggregate the performances of all the indicators into a composite sustainability index by the linear aggregation method by **Eq. (9)** [27].

$$CSI = \sum_{i=1}^{n} CS_j \times w_j \tag{9}$$

where CS_j represents the normalized value of *j*th indicator. In this framework, minimum-maximum method is applied to achieve the normalization further removing the unit influences of indicators based on the reference [27]. Specifically, **Eq. (10)** is used for the normalization of beneficial indicators like the efficiency and profit while those cost indicators like the capital cost and carbon emissions are transformed by **Eq. (11)**.

$$CS_j = \frac{A_j \text{ - } \min A_j}{\max A_j - \min A_j} \tag{10}$$

$$CS_j = \frac{\max A_j \text{ - } A_j}{\max A_j - \min A_j} \tag{11}$$

where A_j represents the actual value of each specified indicator, CS_j is the normalized value of jth indicator. The minimum A_j and maximum A_j are estimated based on the optimization with total annual cost (TAC) as the objective.

2.2 Optimization of configurations

Three alternative ED configurations represented by conventional extractive distillation (CED), side-stream extractive distillation (SED) and thermal-coupled extractive distillation (TED) are considered firstly to achieve the effective separation of EtOH and EtPA. One of the premises to optimize the CSI is to get the minimum and maximum value of determined indicators (see **Eq. (10)** and **(11)**). Therefore, an optimization with the total annual cost (TAC) objective is carried out firstly to estimate the minimum and maximum values for constructing the CSI. The optimization method is the same as the procedure of optimizing the CSI objective.

The optimization model isa mixed integer nonlinear programming (MINLP) problem. However, the derivatives of the objective functions and constraints are not available since the process model is built in Aspen Plus. Therefore, the conventional derivative-based optimization algorithm for MINLP problems are not applicable in this study and a derivate-free optimization algorithm has to be adopted here. One of the effective optimization algorithms to solve the problem is the MADS algorithm [49]. And the NOMAD optimization package developed by previous researchers [50] that has embedded MADS algorithm in it can solve the problem in this work. A pseudo-code of MADS from the user guide of the NOMAD website [35] is shown in **Table 2**.

Table 2. The pseudo-code of the typical MADS [35, 49, 50]

Initialization: Let $x_0 \in R^n$ be an initial feasible solution and set the iteration counter $k \leftarrow 0$

repeat
  Search on the mesh to find a better solution than x_k
    If the search failed, then
    poll on the mesh to find a better solution than x_k

If a better solution than x_k was found by either the search or the poll, then
call it x_{k+1} and coarsen the mesh
Else
set $x_{k+1} = x_k$ and refine the mesh
Update parameters and set $k \leftarrow k+1$
until stopping criteria is satisfied

The whole optimization for these configurations is demonstrated in **Fig. 2**. The programming calling connection between the simulation and optimization tool is achieved by component object model (COM) technology [51]. MADS will then randomly search for a set of solutions around the current point and execute the optimization as illustrated in **Table 2**. Because the maximum iteration number is set to be an extremely big number (1E+09 was used in this study), the iteration will be stopped when the final objective value is within the specified tolerance. Through the continuous iteration calculation, the optimal solution can be identified eventually. And the overall optimization procedure was carried out on a 64-bit desktop computer with an Intel(R) i5-4200H four-core CPU @ 2.8 GHz, including an 8GB RAM.

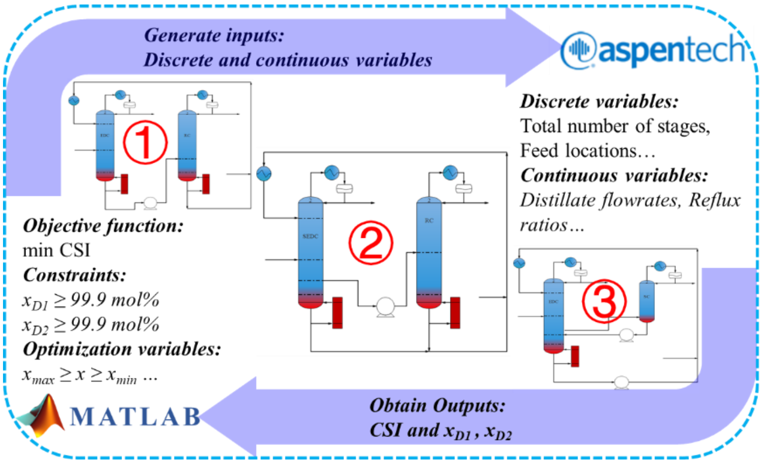

Fig. 2. The MADS optimization procedure for three separation configurations

2.3 Heat-pump distillation design

Various heat-pump schemes can be successfully used in conjunction with distillation and among them mechanical vapor recompression (MVR) type is widely studied [10]. MVR is featured by applying the process fluid itself as the working fluid for vapor recompression. In this way, MVR heat pump could upgrade the heat from the top of the distillation column and reutilize the upgraded heat at the bottom reboiler of the column. Eventually, the total utility heat energy can be reduced, and the low-grade energy of the vapor steam from the top of distillation column can be recovered.

Whether the MVR distillation design is appropriate or not depends on the temperature lift from the heat source to the heat sink. For example, when the temperature difference is too large, the compressor consumes more electricity to upgrades the low-level energy, which represents more operating and equipment cost. It implies that there is a trade-off between the reduced utility energy supply and increased heat-pump devices investment. Therefore, the feasibility analysis of using heat pump should be firstly carried out. Pleşu *et al.* [52] proposed an evaluation criterion Q/W to judge whether a heat pump is worth being implemented to improve the distillation design. As shown in **Eq. (12)**, Q/W is the ratio of the heat rejected (Q) at high temperature to the required work (W) of the compressor.

$$\frac{Q}{W}=\frac{1}{\eta_C}=\frac{T_C}{T_R\text{-}T_C} \tag{12}$$

where η_C is Carnot efficiency. The temperature of the condenser and reboiler is denoted by T_C (K) and T_R (K), respectively. According to the work by Zhang *et al*. [53], the heat pump is strongly recommended when Q/W is higher than 10. It should be mentioned that the condenser and the reboilerdiscussed in **Eq. (12)** may not come from the same distillation column. Besides, temperature-enthalpy (T-H) diagrams can have a clear representation for such heat integration achieved by upgrading the heat level of the top vapor stream [54]. The overall hot and cold requirements in a heat-integration process are fully observed via the hot composite curve (*i.e.,* HCC) and cold composite curve (abbreviated as CCC) in the T-H diagram. The overlap regions between HCC and CCC represent the amount of heat recovered in the process.

2.4 Multi-criteria sustainability indicators

As it has been shown in the sustainability metrics introduction [55], three basic groups (i.e., environmental, economic and social indicators) are generally considered in the sustainable chemical engineering design. Because of the variety of sub-indicators in different aspects, three major criteria are considered here in the selection of the sustainability indicators. The first one is that indicators selected should be measurable or quantitative. For example, some indicators under the social sustainability are hard to be quantified and we have to select the appropriate one to reflect the social sustainability performance. Next, indicators in one aspect can sufficiently describe the corresponding sustainability performance. This means that, for example, cost and benefit indicators should be included to describe the economic performance. The last one is that sub-indicators that related decision-makers are significant for the project should be selected. Also, sustainability research in the chemical process engineering domain has used various sub-indicators for process retrofitting [56, 57].

We finally determined the sustainability sub-indicators based on the above-mentioned criteria meanwhile considering the feature of the distillation process. Those sub-indicators widely used before in distillation process design were selected at our priority [16, 58, 59]. And detailed description has been given in the following subsections.

2.4.1 Economic evaluation

In this study, the total annual cost (TAC) is applied to assess the economic performance of proposed processes which is calculated by the sum of annual energy consumption and equipment investment as shown in **Eq. (13)**.

$$TAC = \frac{TCC}{payback\ period} + AEC \tag{13}$$

Where TCC represents the total equipment investment including the major cost of distillation columns, heat exchangers and compressors. Other additional fittings like pumps and pips are generally neglected owing to their lower cost compared to the columns. Moreover, the payback period is assumed to be 5 years and 7200 hours each year [53]. Throughout the calculation, the utility consumptions such as electricity, cooling water and steam under different pressures are supplied and the annual energy cost is represented by AEC. Based on the reference [60], detailed equations and specified parameters for the economic cost evaluation are shown as below.

$$h(m) = 0.6096 \times (N_T - 2) \times 1.2$$

(14)

$$Column\ shell\ cost\ (\$) = \left(\frac{M\&S}{280}\right) \times CSc \times d^{1.006} \times h^{0.802} \tag{15}$$

$$Column\ tray\ cost\ (\$) = \left(\frac{M\&S}{280}\right) \times 97.243 \times d^{1.55} \times h \times 1.4 \tag{16}$$

Where N_T represents the number of trays for each column, *h* is the column height and *d* donates the dimeters of each column. The applied value of Marshall & Swift index (*M&S*) is 1468.6 [61]. *CSc* is the coefficientdetermined by the operating pressure ranges shown in **Table S1**.

$$Reboiler\ cost\ (\$) = \left(\frac{M\&S}{280}\right) \times \left(\frac{Q_R}{U_R \times \Delta T_R}\right)^{0.65} \times Ch \tag{17}$$

$$Condenser\ cost\ (\$) = \left(\frac{M\&S}{280}\right) \times \left(\frac{Q_C}{U_C \times \Delta T_C}\right)^{0.65} \times Ch \tag{18}$$

Hereafter we use Q (kW) to represent the duty of reboilers and condensers in distillation columns, U represent the heat transfer coefficient and ΔT (K) is the temperature difference. Subscripts R and C denote functions and variables relevant to the calculation of reboiler and condenser. U_R and U_C are assumed to be 0.568 kW/K.m^2 and 0.852 kW/K.m^2 respectively [62]. The cost of heat exchangers is different according to the condenser and type of reboilers, which is expressed by the coefficient value Ch (see **Table S2**). Both **Tables S1** and **S2** are consistent with the work of Olujić *et al.* [60].

$$Compressor\ cost\ (\$) = \left(\frac{M\&S}{280}\right) \times 2047.24 \times \left(\frac{W}{0.72}\right)^{0.82} \tag{19}$$

$$Energy\ cost\ (\$) = \left(Cs \times Q_R + Cc \times Q_C + \left(\frac{W}{0.72}\right) \times Ce\right) \times 7200 \tag{20}$$

Where W (kW) represent the brake work of the compressors. The efficiency of compressors is assumed as 72%. In terms of the calculation of cost by energy consumptions, Cs, Cc, and Ce denote the utility price of steam, cooling water and electricity. Only cooling water is considered in the condenser since the temperature of distillates is much higher than 313.15 K. The price of the utilitiesis listed in **Table S3**.

In addition, to evaluate the selling profit of the pure products within different the proposed separation schemes, the total annual revenue (TAR) based on **Eq. (21)** is calculated [63].

$$TAR(\$) = \left(\sum_{t=0}^{n} \frac{CF_t}{(1+r)^t}\right) \Big/ n \tag{21}$$

Where CF_t stands for the cash flow in the current year t and r represents the discount rate 5%. In this study, we assume the n is equal to 5 to evaluate the total net profit in annual year and the cost of the mixture equals to the waste treatment cost 0.0012 \$/kg [59]. The price of other solvents like EtOH, EtPA and IBAC are 1.03 \$/kg, 10.87 \$/kg and 18.26 \$/kg respectively according to the market [64]. The uncertainty of selling demand and market fluctuation is ignored in the estimation.

2.4.2 Environmental impact

Steams of various pressures are supplied to reboilers for heating purpose in distillation operation while compressors consume large quantities of electricity . Both reboilers and compressors are significant energy consumers and emission contributors. Note that emissions are not directly generated during the separation process but indirectly come from the procedures of energy supply [65]. For example, steam can be produced by burning specified types of fuels such as coal, heavy oils and natural gas which may generate much greenhouse gas and otherpollutants. In this work, the amount of CO_2, SO_2 and NO_x emissions are assumed to be environmental indicators and coal is set as the primary fuel for the simplicity of calculation. The energy from consumed steam is firstly converted into the amount of standard coal as shown in **Eq. (22)**. Then the total emissions of CO_2, SO_2 and NO_x expressed by **Eq. (23)** can be calculated according to the standard coal conversion factor and electricity conversion factor [66].

$$M_{coal}(kg) = \frac{Q_R \times T}{Q_{standard}} \tag{22}$$

$$Emission(kg) = a \times M_{coal} + b \times W \tag{23}$$

Where Q_R (KW) is the heat duty of reboilers, T is equal to 7200 hours as the operation time in a year. $Q_{standard}$ stands for the net heat value of the standard coal, which is 29307.6 kJ/kg. W (kW) represents the brake work of the compressors. Besides, a and b correspond to the emission conversion factor of standard coal and electricity, which is summarized in **Table S4** [67].

2.4.3 Safety evaluation

The fire and explosion damage index (FEDI) proposed by Khan and Abbasi [68] is applied to evaluate the inherent safety in the distillation process since it can systematically consider the influence from the pressure, temperature, equipment and chemicals. In this work, we focused on the FEDI of the distillation columns while other equipment like pips, pumps and compressors that have lower stream handling are neglected in the calculation. Note that the total process safety is determined by the most hazardous unit with the largest FEDI value. The calculation has been shown in the following equations featured by no reactions and a detailed description can be found in the reference [68, 69].

$$FEDI = 4.76 \times (damage\ potential)^{0.333} \tag{24}$$

$$damage\ potential = (F_1 \bullet Pn1 + f(F_2, F_3) \bullet Pn2) \times (Pn3 \bullet Pn4 \bullet Pn5 \bullet Pn6) \tag{25}$$

Where F stands for different energy factors and Pn represents the penalties value according to the condition of pressure, temperature, and the quantity of the chemicals in the specified equipment. For the distillation unit the damage potential is calculated by the **Eq. (25)**. And detailed information and parameter selection for the considering distillation columns are described in Appendix. A.

2.4.4 Energy utilization efficiency

In this study, the thermodynamic second-law efficiency (η) is calculated to assess the energy utilization performance. Seader *et al.* [70] has proposed a method for the calculation of the second-law efficiency.

$$\eta = \frac{W_{min}}{LW + W_{min}} \tag{26}$$

$$LW = \sum_{in}(nEx + Q(1 - \frac{T_0}{T_S})) - \sum_{out}(nEx + Q(1 - \frac{T_0}{T_S})) \tag{27}$$

$$W_{min} = \sum_{out} nEx - \sum_{in} nEx \tag{28}$$

Where W_{min} (kJ/h) indicates the minimum work of achieving the separation task and LW is the lost work (kJ/h). In addition, n represents the stream flowrate (kmol/h) in the system. The temperature and heat duty of heat source and sink are indicated by T_S and Q, respectively. An infinite source or sink for heat transfer at the absolute temperature T_0 (298.15K) of the surroundings is defined. Ex (kJ/kmol) denotes the exergy of stream flow into or out of the system.

3. Computational results

3.1 Entrainer selection

According to the little shift and pinch point appearance in azeotropic composition (see **Fig. S1** in Appendix. A) under the pressure-swing condition increasing from 1 atm to 5 atm or decreasing from 1 atm to 0.2 atm, it is not a good choice to apply pressure-swing distillation to the separation of EtOH and EtPA. In this study, we focus on the extractive distillation scheme to achieve the effective separation of EtOH and EtPA. Herein, NRTL was selected as the thermodynamic model since it can fit the experimental data well [36]. In the design of the extractive distillation, entrainer determination influence the extractive efficiency and the total energy consumption. Four candidate entrainers like isobutyl acetate (IBAC), dimethyl sulfoxide (DMSO), N,N-dimethylformamide (DMF) and N-methyl pyrrolidone (NMP) are considered since they were commonly used solvents to break the azeotrope in the ED processes [71, 72]. The binary parameters of the NRTL model for EtOH-IBAC and EtPA-IBAC are not available within Aspen Plus inbuilt database, hence the binary parameters of both are obtained from the experimental research and regression parameters of Song *et al.* [37]. Some other binary parameters of NRTL (*i.e.,* EtOH-NMP, EtPA-DMSO, EtPA-DMF, EtPA-NMP) have not been explored and collected in the open literature and UNIFAC was used to estimate the missing data. And all binary parameters of the studied system are summarized in **Table 3**.

Table 3. Binary parameters for the four candidate entrainers with EtOH-EtPA

Component i	Component j	a_{ij}	a_{ji}	b_{ij} (K)	b_{ji} (K)
EtOH	EtPA	0	0	398.010	-16.592
EtOH	IBAC	1.626	3.300	-498.551	-880.721
EtPA	IBAC	-8.891	1.855	3987.290	-1150.060
EtOH	DMSO	0.451	0.093	8.126	-249.715
EtOH	DMF	-4.892	-4.792	3295.421	915.836
EtOH	NMP	0	0	-333.520	-207.297
EtPA	DMSO	0	0	322.925	275.590
EtPA	DMF	0	0	329.503	-56.293
EtPA	NMP	0	0	108.684	45.036

The ternary system that consisting of binary azeotropic mixture EtOH-EtPA and another heavy entrainer was recognized as the 1.0-1a type topological structure (see **Fig. S2**). And all types of feasible topological structures for ternary mixtures have been summarized in the reference [73]. By combining the residue curves and univolatility curves shown in the ternary diagrams namely residue curve maps (RCMs), essential information could be obtained while making a conceptual design of the special distillation systems. The RCMs of the ternary system EtOH-EtPA mixture with another entrainer (*i.e.,* IBAC, DMSO, DMF, NMP) has been presented in **Fig. 3**. It is worth noting that **Fig. 3. (a)** and **(c)** stand for the result that adding entrainer increases the relative volatility of EtOH-EtPA (*i.e.,* $\alpha_{A/B} > 1$). In contrast, as shown in **Fig. 3. (b)** and **(d)**, by adding DMSO or NMP into the system, the relative volatility of EtOH-EtPA is altered to be less (*i.e.,* $\alpha_{A/B} < 1$) since the univolatility curve intercepts the EtPA/entrainer edge of the triangle. Therefore, the smaller the distance between the x_P point to the separated components (*i.e.,* EtOH and EtPA) the more effective the entrainer is. IBAC is eventually selected owing to the smallest distance of the x_P point. We then checked the relative volatility between EtOH and EtPA after the entrainer IBAC has been added, which was presented in **Fig. S3** of Appendix. A. It further validated that IBAC can well break the azeotrope between EtOH and EtPA mixture.

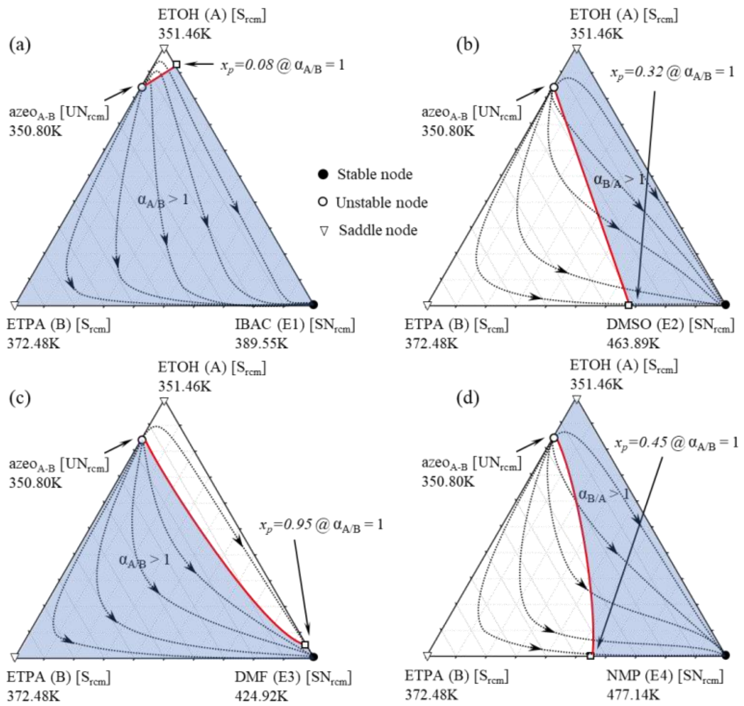

Fig. 3. RCMs of the EtOH-EtPA mixture with four candidate entrainers at 1 atm

3.2 Construction of CSI

Four representative indicators including the TAC, TAR, TCC and AEC are used for measuring economic sustainability. Since the TCC and AEC are already included in TAC, there is no need to consider TAC in the CSI construction again. CO_2, SO_2 and NO_x emissions are used as the environmental indicators to address the environmental sustainability of distillation processes. The thermodynamics second law efficiency η of distillation processes is used for technical evaluation. Moreover, the FEDI is calculated to assess the process inherent safety. The smaller the FEDI, the better the chemical processes will be [68]. In summary, eight indicators in four categories are used for sustainability assessment (See **Table 4**).

Table 4. Criteria for the construction of the composite sustainability index

Aspects	Economic (AS1)	Environmental (AS2)	Technical (AS3)	Social (AS4)
Indicators	TAR (C1)	CO_2 emission (C4)	η (C7)	FEDI (C8)
	TCC (C2)	SO_2 emission (C5)		
	AEC (C3)	NO_X emission (C6)		

The fuzzy comparison matrix of the four aspects (*i.e.,* AS1, AS2 AS3, AS4), the economic indicators (*i.e,* C1, C2, C3), and the environmental indicators (*i.e.,* C4, C5, C6) have been presented in **Tables S7, S8 and S9**. By solving the constrained nonlinear model as shown in **Eq. (5)** in section 2.1, the fuzzy weights of individual indicators can be obtained. And then we can get the defuzzied weights by **Eq. (6)**. The global weights of the eight indicators are determined by the product of the corresponding local weight and the weight of the corresponding aspect. For example, the global weight of the C1 indicator (*i.e.,* 0.1454) can be calculated by the product of the local weight of the AS1 (*i.e.,* 0.3639) and the local weight of C1 (*i.e.,* 0.3996). All the obtained weighting results have been presented in **Table 5**. It can be seen the safety has the highest weight in this case and it indicates the highest priority was given to the safety in distillation operation. Environmental impact was represented mainly by CO_2 emission C5. The economic performance is dominated by the TAR and TCC with the same weight of 0.1454.

Table 5. The weights of nine specified indicators and four-dimension aspects

Indicators	Fuzzy weight			Defuzzied weight	Global weight
	w^L	w^M	w^U		
AS1	0.3103	0.3636	0.4185	0.3639	-
C1	0.2807	0.3425	0.4005	0.3996	0.1454
C2	0.2605	0.3256	0.3882	0.3996	0.1454
C3	0.1986	0.2143	0.2335	0.2008	0.0732
AS2	0.2098	0.2770	0.3591	0.2217	-
C4	0.5588	0.5745	0.5745	0.5719	0.1598
C5	0.1711	0.2056	0.2463	0.2066	0.0577
C6	0.1792	0.2200	0.2701	0.2215	0.0619
AS3	0.1340	0.1343	0.1379	0.1349	-
C7	0.1340	0.1343	0.1379	0.1349	0.1349
AS4	0.1932	0.2251	0.2369	0.2217	-
C8	0.1932	0.2251	0.2369	0.2217	0.2217

Based on the obtained weights, a linear aggregation method is applied to construct the CSI objective. The maximum and minimum values of each indicator should be estimated by optimizing TAC objective function. It is worth mentioning that some indicators' values in the optimization of CSI may not locate in the same space of the minimum and maximum results in the optimization of TAC, therefore the space obtained from the optimization of TAC was expanded by 30%. For instance, if the minimum and maximum value of TAR from the TAC optimization are 100 and 200, then we estimate the applied minimum and maximum value for calculating CSI are 70 and 260. **Tables S10**, **S11** and **S12** have listed those values for the CSI calculation of three ED configurations, respectively. Applying the normalization method mentioned in section 2.1, the CSI can be calculated in the Aspen Plus according to **Eq. (9)**.

3.3 Optimization with CSI objective

In this work, the fresh feed condition and recycled temperature are the same as the simulation initial results by Song *et al.* [37], namely the flowrate of fresh feed is 100 kmol/h with an equivalent molar fraction of EtOH-EtPA and the temperature of fresh feed and the recycled stream is set as 323.15 K and 360.15 K. Operating pressures of each distillation column are 1 atm with single tray pressure drops of 0.0068 atm. All the proposed configurations have the same separation requirement that products purities are no lower than 0.999 with molar fraction.

3.3.1 Conventional extractive distillation

In terms of the CED, decision variables such as the total number of stages of two columns (NT_1 and NT_2), the locations for the feed streams (NF_1 and NF_2) and recycled entrainer (N_E), the molar flowrates of the distillates (D_1 and D_2), the reflux ratios (RR_1 and RR_2) and the flowrate of the recycled entrainer (F_E) need to be optimized. When setting the lower and upper bounds of decision variables, it is a prerequisite to ensure the final parameters of optimal decision variables are not the boundary values. To achieve this goal, multiple trials and optimization adjustments must be carried out. **Table S13** in the Appendix has listed the final bounds of decision variables including five discrete variables and five continuous variables. It is worth noting that whether low-pressure steam or middle-pressure steam is provided in the reboiler depends on the bottom temperature of the columns. Therefore, selecting varied steam prices to calculate the cost is coded in the "Calculator" of Aspen Plus by some if-loops. This programming ensures that the algorithm in Matlab can find the correct optimized conditions automatically.

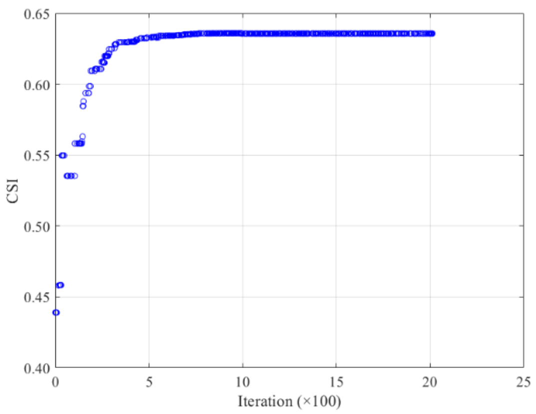

Fig. 4. The optimization variation of CSI with an increasing iteration of the CED process

Some unexpected results or errors maybe turn up during the optimization procedure. For example, the obtained feed location NF_2 is larger than the total number of stages NT_2. And the other problems are the emerging warnings and errors in the simulation running. Thus, to overcome the above-mentioned problems, a large penalty cost function was given to the CSI value and the simulation could be reinitiated. The applied method in major programming guarantees the process convergence and solution accuracy. And the optimization variation of CSI for the CED process with increasing iteration number has been displayed in **Fig. 4**. It took 3.61 hours to obtain the optimal results until the mesh size reaches the stop criterion of NOMAD programming. Thereduction of CSI is marginal after 1000 iterations,which means the solution is finally obtained.

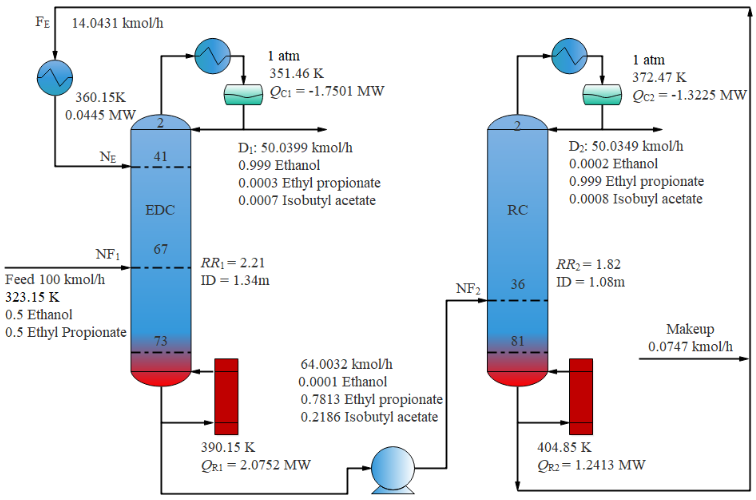

Fig. 5. Optimal CED process flowsheet with detailed information

The optimal CED process along with detailed parameters has been shown in **Fig. 5**. The first distillation column has 74 stages with a reflux ratio of 2.21 while the recovery column has 82 stages with a lower reflux ratio of 1.82. In addition, the liquid composition and temperature profile are presented for the optimal CED process in **Fig. S4**. It is evident from **Fig. 5** that there is little difference between the temperature of the reboiler (390.15 K) in the extractive distillation column (abbreviated as EDC) and the temperature of the condenser (372.47 K) in the recovery column (*i.e.,* RC). Reasonable consideration is either to increase the pressure of RC or reduce the pressure of EDC to make a heat-integration design between two columns. We analyzed the RCMs of the EtOH-EtPA-IBAC (see **Fig. S5**) to explore why increasing the pressure of RC or decreasing the pressure of EDC to achieve heat integration is not suitable. As shown in **Fig. S5(a)**, when the operation pressure of EDC decreases the x_p point moves far away from the EtOH product which means the extractive effect of the entrainer is not as good as that in 1 atm. In addition, the *x-y* diagram of EtPA and IBAC has been displayed in **Fig. S5(b)**. The pinch is formed when pressure increases to 2 atm and the azeotrope appears when the pressure increased to 5 atm. It represents the separation of the high-purity IBAC or

EtPA in a single RC is harder when the pressure increases. Above all, the energy-saving heat-integration design cannot be realized by the pressure-swing method.

3.3.2 Side-stream extractive distillation

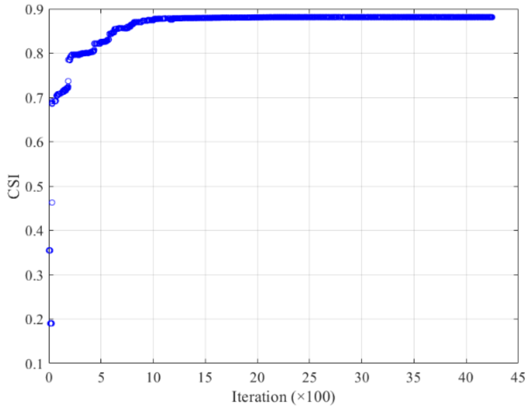

Fig. 6. The optimization variation of CSI with increasing iteration for the SED process

Inspired by the innovative study [74], the side-stream extractive distillation (SED) configuration was also applied on the separation of EtOH-EtPA targeting on possibly searching for a more energy-saving scheme.In addition, our previous study [75] concludes that once a part of entrainer is imported from the bottom of EDC, the energy consumption of RC will be greatly cut back. Therefore, a similar optimization procedure is carried out for the SED process and pressures of both distillation columns are fixed at 1 atm. Parameters such as the total number of stages (N_{T1}, N_{T2}), the locations of the feed streams (NF_1, NF_2) and recycled entrainer (N_E), the molar flowrate of the distillates (D_1, D_2), the reflux ratios (RR_1, RR_2) and the flowrate of the recycled entrainer (F_E) are the decision variables. The location (N_S) and flowrate (F_S) of side discharged stream need to be determined. In summary, six discrete and six continuous decision variables for the SED design are considered and the corresponding bounds for the optimization process are listed in **Table S14** of the Appendix. A.

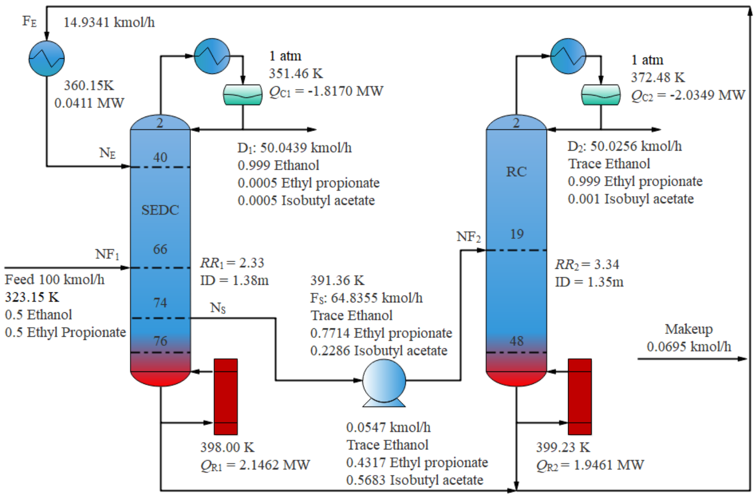

Fig. 7. Optimal SED process flowsheet with detailed information

The optimization variation of CSI for the SED process with increasing iteration number has been presented in **Fig. 6**. And it lasts for 12.28 hours to stop the optimization solver. Eventually, a set of optimal design variables meeting the purity constraints and maximized CSI are obtained, and detailed information has been shown in **Fig. 7**. The first distillation column has 77 stages with a reflux ratio of 2.33 while the recovery column has 49 stages with a larger reflux ratio of 3.34. The obtained TAC for the SED process after the maximization of the CSI is 1.18×10^6 \$/year. The detailed comparison and analysis for the phenomenon that the SED configuration shows larger TAC than CED will be given in section 4. In addition, the liquid composition and temperature profile are presented in **Fig. S6** for the optimal SED process.

3.3.3 Thermal-coupled extractive distillation

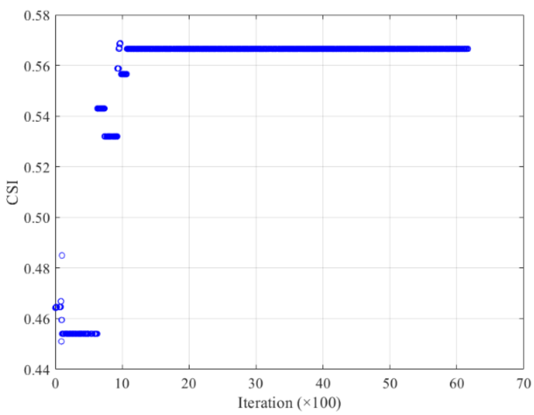

Fig. 8. The optimization variation of CSI with increasing iteration for the TED process

Thermal-coupled extractive distillation (TED) has been investigated since it is effective to overcome the remixing problem in some specified separation systems [76, 77]. Therefore, TED is another proposed configuration expecting to achieve a more energy-saving design in the separation of EtOH-EtPA. Parameters such as the total number of stages (NT_1, NT_2), the feed locations of the fresh feed stream (NF_1) and recycled entrainer (N_E), the molar flowrate of the distillate (D_1, D_2), the reflux ratio (RR_1) and the flowrate of the recycled entrainer (F_E) are set as the decision variables. In addition, variables like the location (N_{SO}) and flowrate (F_{SO}) of the side stream discharged from EDC also need to be determined. The location of the input stream (N_{SI}) that fed into the EDC is the same as N_{SO}. And the location of the output stream (NF_{SO}) that fed into the RC is equal to NT_2. The above equations can be summarized as follow:

$$NT_1 < N_{SO} \tag{27}$$

$$N_{SO} = N_{SI} \tag{28}$$

$$NT_2 = NF_{SO} \tag{29}$$

In summary, a total of five discrete variables (*i.e.*, NT_1, NT_2, NF_1, NF_E, and N_{SO}) and five continuous variables (D_1, D_2, RR_1, F_E and F_{SO}) for the TED design are first considered. All decision variables and their bounds are listed in **Table S15**. Eventually, we finished the optimization of TED scheme in 14.26 hours. **Fig. 8** presents the variation of objective function CSI with increasing iteration number for the TED configuration.

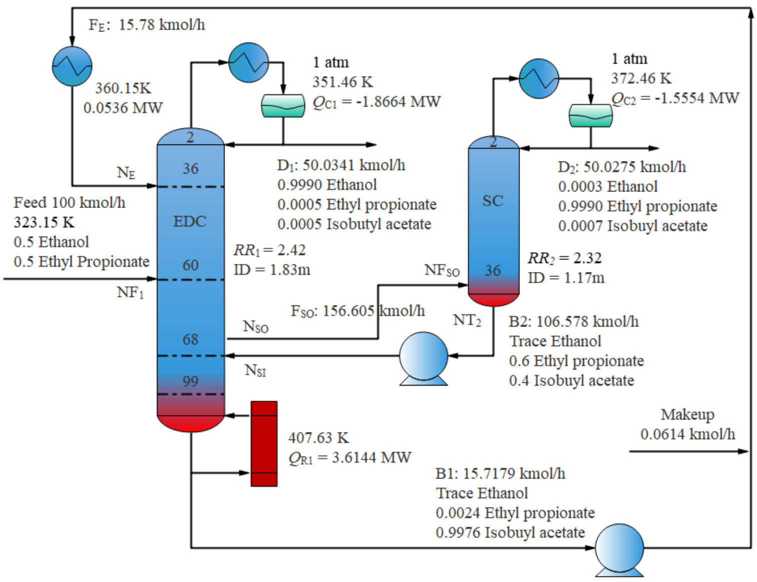

Fig. 9. Optimal TED process flowsheet with detailed information

Detailed TED process flowsheet with optimal results has been shown in **Fig. 9**. The total number of stages of the major column is 100 and the side rectifier column has 36 plates. Only one reboiler is used in the design but it has not improved the economic performance too much. The optimal TAC for the TED process under the maximum CSI is 1.17×10^6 \$/year which is slightly smaller than that of SED. Also, the liquid composition and temperature profile are presented for the optimal TED process in **Fig. S7** in the Appendix. A. The final optimization result does not meet the expectation that it can overcome the remixing problem and reduce the total energy consumption. A detailed analysis has been given in section 4.

3.4 Heat-pump distillation design

Based on the optimal separation configuration CED with the best sustainability performance (see **Fig. 14**), the heat pump technique is considered to guide the upgrading design of CED process. As explained before in section 2.3, the heat-pump assisted CED can be economically considered when the Q/W is greater than 10. As shown in **Fig. 5**, the Q/W of EDC is calculated to be 9.1 since temperatures of condenser and reboiler are 351.46 K and 390.15 K, respectively. The Q/W of RC is 11.5 according to the fact that the temperatures of condenser and reboiler are 372.47 K and 404.85 K. And the Q/W with 21.1 is obtained based on temperatures of RC condenser (372.47 K) and EDC reboiler (390.15 K). Standing for the view of economic cost, two heat-pump assisted CED systems are proposed owing to the larger Q/W (*i.e.,* 11.5 and 21.1).

3.4.1 Heat-pump assisted CED with different columns

The first heat-pump scheme is to transfer heat from the top steam of RC to the bottom reboiler of EDC based on the Q/W value of 21.1, which is termed as heat-pump assisted CED with different columns (*i.e.,* HCED-D). During the design of HCED-D, the discharge pressure of the compressor is a key variable that influences the CSI of the process. Also, some preheaters in the heat-integration design are applied to improve the compression efficiency and the minimum heat transfer temperature difference of the preheaters remains to be 10 K. The synthesis of HCED-D scheme is simulated in the Aspen Plus as follow:

1. Fix the total number of stages, reflux ratios and distillates flowrates.

2. The vapor stream leaving from the RC is introduced firstly into Preheater 1 while keeping the temperature difference between S2 and S4 stream is 10 K.

3. S2 stream is connected to the compressor and vapor S3 stream after compressed is introduced into another heat exchanger (see Reboiler 2) which is used to boil the bottom stream of EDC. The purpose of Reboiler 1 is to keep the S4 stream fully vaporized and transfer heat to the bottom stream.

4. To find the optimal discharge pressure of the compressor, a new design specification by Design Spec/Vary function is applied to meet the minimum temperature difference of heat transfer.

5. S4 as the heat source stream is connected to Preheater 1 with countercurrent flow direction, the leaving heat source stream S5 flows into Preheater 2 and discharged S6 stream is cooled to 372.47 K which exactly is the condenser temperature of EtPA with 0.999 molar fraction.

6. Calculate the resulting compressor work duty and the reboiler heat exchanger duty.

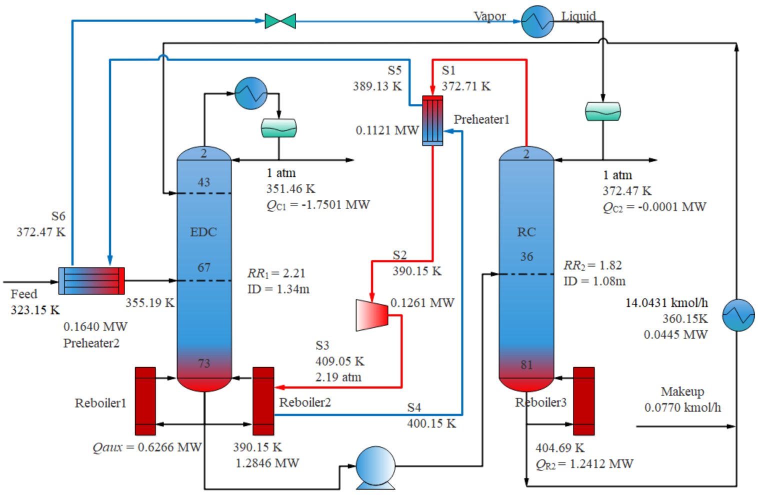

Fig. 10. The improved HCED-D scheme for the separation of EtOH-EtPA

Through the procedure mentioned above, the detailed heat-integration results of the improved HCED-D scheme were presented in **Fig. 10**, and the discharged pressure of the compressor is 2.19 atm. And it is observed that upgrading S3 stream achieves the partial heat transfer to one reboiler by releasing its full latent heat of 1.2846 MW. Liquid stream S4 with low-grade energy can be further reused for heating the S1 and fresh feed stream by two preheaters. It is apparent that the utility energy consumption of EDC has been reduced to 0.6266 MW. **Fig. 11** illustrates the T-H diagram of the improved heat-pump distillation design. It can be observed that an overlap region in the plot stands for the heat recovery zone in the heat-pump design.

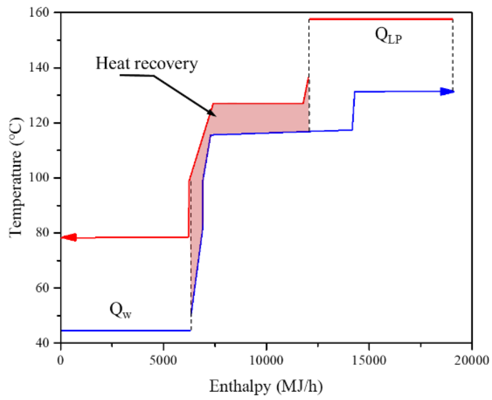

Fig. 11. The T-H diagram of HCED-D scheme for the separation of EtOH-EtPA

3.4.2 Heat-pump assisted CED in a single column

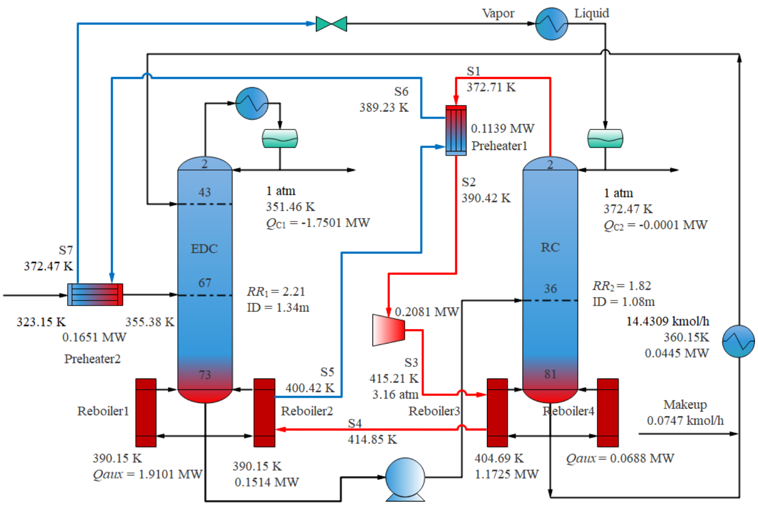

Fig. 12. The improved HCED-S scheme for the separation of EtOH-EtPA

Another improved configuration with the heat-pump technology is to transfer heat from the top of the RC to supply the RC reboiler firstly. This upgrading process is termed as the HCED-S scheme. The synthesis of the HCED-S is obtained with a similar procedure to that in HCED-D. The obtained HCED-S with a detailed heat-integration design is demonstrated in **Fig. 12**. The pressure of the discharged stream from the compressor is 3.16 and discharged stream S4 with high temperature could be further used to reduce the steam consumption of EDC. Eventually, it can be calculated that the recovered heat energy in the reboiler equals to 1.3238 MW. As shown in **Fig. 13**, the heat-integration design in HCED-S has a much larger overlap region, which means more steam energy has been saved.

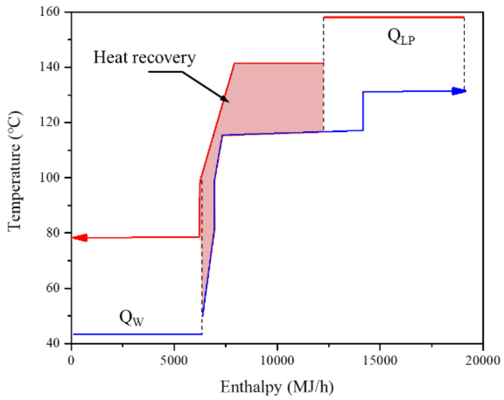

Fig. 13. The T-H diagram of HCED-S scheme for the separation of EtOH-EtPA

4. Multi-criteria sustainability analysis

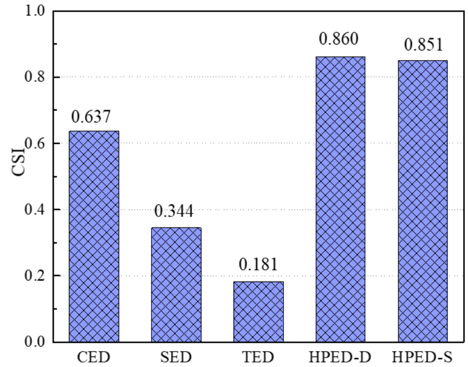

Fig. 14. The calculated CSI of different extractive distillation schemes

The detailed values of multiple sustainability aspects of the five proposed separation schemes are listed in **Table S16**. To give a direct comparison in sustainability, the maximum and minimum values of each indicator were selected, and the CSI values of each process scheme were calculated. The final CSI results based on the determined pairwise comparison matrix have been presented in **Fig. 14**. According to the results, HCED-D is the most sustainable design for the separation of EtOH-EtPA azeotropic mixture under the obtained weights. The illustration of indicators value is compared in **Fig. 15**. The beneficial indicators are presented with a negative value. Comparing with the TED scheme, the HCED-D has a reduction of TAC by 21.09% and CO_2 emission by 48.32%. The energy utilization efficiency η of HCED-D has been greatly increased by 80.32 % because a huge amount of energy has been recovered by heat-pump technology. In addition, TAR values for the CED, HCED-D and HCED-S schemes differ little because EtOH and EtPA products show much higher selling prices although the investment cost varied. Market price fluctuation and selling amount was neglected in this study. Three configurations of CED, HCED-D and HCED-S show the same FEDI for which the FEDI is determined by the most dangerous equipment. And the FEDI value of added compressor is lower than the distillation columns.

Both improved heat-pump schemes (*i.e.,* HCED-D and HCED-S) have a lower energy consumption while a larger capital cost compared with the CED process. This means that the energy recovery was achieved with the cost of increasing the equipment investment. In other words, it is easy to achieve heat integration and energy saving by implementing heat-pump technology, however one consideration is the compromise between increasing capital cost and reducing energy cost. A detailed explanation about the trade-off in this case study has been given in **Fig. S8**.

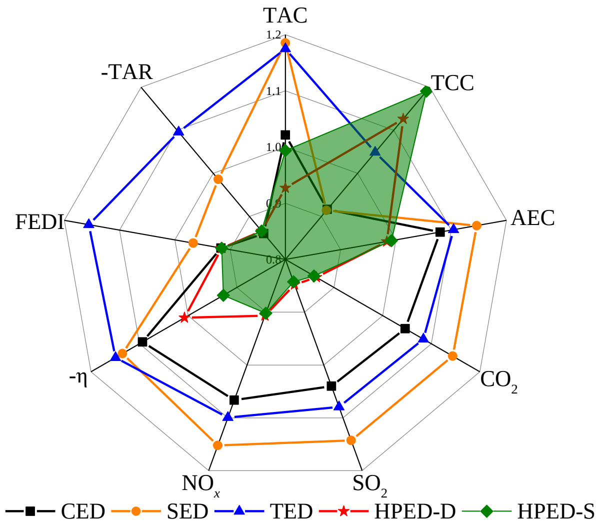

Fig. 15. The comparison radar diagram of different schemes

Noting the SED scheme does not show any superiority over CED in any aspects, which is quite different from what researchers have done before [65]. We then paid attention to the reboiler duty of the two distillation columns in SED and found that only a small flowrate stream (*i.e.,* 0.055 kmol/h) is discharged from the bottom of the first column. This is not a good phenomenon for saving energy, because it represents bad separation effects in the stripper section of the first distillation column. As shown in **Fig. 5**, the purity of the IBAC in the bottom stream of EDC is only 56.83%, which implies the discharged amount of the bottom stream cannot be large otherwise the total recycled stream is not pure enough to ensure the process convergence. In other words, much more plates in the first distillation column of SED than that of CED do not achieve the expected separation effect to obtain enough amount of recycled entrainer. This costly configuration of SED has been reflected on the bad economic performance. Above all, using SED scheme for the separation of specified mixture EtOH-EtPA is not suitable. Also, applying the TED configuration for separating EtOH-EtPA is not a good choice. One major reason is the total steam energy consumption of TED is larger than that of CED process. To better analyze the phenomenon, the composition profiles of the CED and TED configurations have been presented in ternary diagrams (see **Fig. S9**). It can be observed from **Fig. S9(b)** that the repeated path is longer, which means the energy consumption of the reboiler in TED is larger than that of CED configuration to reach the product purity of 99.9 mol%.

5. Conclusions

In this work, a case study for the separation of azeotropic mixture ethanol-ethyl propionate was performed to illustrate the sustainable distillation design and optimization framework, which includes the construction of a composite sustainability index, stochastic optimization, improved design with heat-pump technique and multi-criteria sustainability analysis. Three extractive distillation configurations (*i.e.,* CED, SED and TED) and two heat-pump distillation design (*i.e.,* HCED-D, HCED-S) are investigated and evaluated from different perspectives of the composite sustainability index namely economic evaluation, environmental impact, energy utilization and safety assessment. Noting that the constructed CSI can provide an optimization guide for multiple sustainability evaluation in the distillation design, simultaneously. The proposed HCED-D scheme has shown the most sustainable result though HCED-S configuration has a good performance as well. Compared with the TED process, the TAC of the HCED-D scheme is reduced by 21.09%, CO_2 emission is decreased by 48.32% , and energy utilization efficiency is increased by 80.32%. However, the proposed framework of improved distillation process design still shows some weaknesses which should be further studied. The first one is about the sustainability comparison matrix since the choice of sustainability indicators may be somewhat subjective. This issue is possible to be overcome by considering different suggestions from multiple decision-makers in practice. Another one is related to the aggregation of a composite sustainability index. Herein, a simple linear aggregation method was used. However, an undesirable feature of this method exists when there are substantially high values of some indicators. In that case, the poor performances of some indicators can be compensated by other indicators. Other aggregation methods like geometric aggregation and non-compensatory multi-criteria approach could be further investiagedin the future. Finally, it could be more interesting and comprehensive to incorporate the computer-aided molecular design method (CAMD) into the selection of extensive candidate entrainers. Our study follows a thought that firstly determining the entrainer using RCMs then assessing the process sustainability performance. The weakness of this entrainer selection method is that the scope of candidate entrainers for screening is narrow and the optimal entrainer may strongly depend on the extractive distillation process conditions.

Author Information

Corresponding Author

E-mail: jzhren@polyu.edu.hk

Declaration of Competing Interest

The authors declare no competing financial interest.

Acknowledgments

The authors would like to express their sincere thanks to the Research Committee of The Hong Kong Polytechnic University for the financial support of the project through the PhD studentship (project account code: RK3P to T. Shi, RK2B to Y. Liu) and this work was financially supported by Joint Supervision Scheme with the Chinese Mainland, Taiwan and Macao Universities - Other Chinese Mainland, Taiwan and Macao Universities (Grant No. SB2S to A. Yang).

Appendix. A

The Appendix A is available free of charge *via* the Internet.

Nomenclature

LLSM	Logarithmic least squares method
CSI	Composite sustainability index
EtOH	Ethanol
EtPA	Ethyl propionate
RCMs	Residue curve maps
TAC	Total annal cost
TAR	Total annal revenue
TCC	Total capital cost
AEC	Annual energy cost
CED	Conventional extractive distillation
SED	Side-stream extractive distillation
TED	Thermal-coupled extractive distillation
MINLP	Mixed integer non-linear programming
MADS	Mesh adaptive direct search algorithm
IBAC	Isobutyl acetate
DMSO	Dimethyl sulfoxide
DMF	N, N-dimethylformamide

NMP	N-methyl pyrrolidone
EDC	Extractive distillation column
RC	Recovery column
HCED-D	Heat-pump assisted CED with different columns
HCED-S	Heat-pump assisted CED in a single column

References

[1] Y. Hu, Y. Su, S. Jin, I.L. Chien, W. Shen, Systematic approach for screening organic and ionic liquid solvents in homogeneous extractive distillation exemplified by the tert-butanol dehydration, Separation and Purification Technology 211 (2019) 723-737. https://doi.org/10.1016/j.seppur.2018.10.030.

[2] W. Shen, L. Dong, S.A. Wei, J. Li, H. Benyounes, X. You, V. Gerbaud, Systematic design of an extractive distillation for maximum-boiling azeotropes with heavy entrainers, AIChE Journal 61(11) (2015) 3898-3910. https://doi.org/10.1002/aic.14908.

[3] Y. Wang, G. Bu, X. Geng, Z. Zhu, P. Cui, Z. Liao, Design optimization and operating pressure effects in the separation of acetonitrile/methanol/water mixture by ternary extractive distillation, Journal of Cleaner Production 218 (2019) 212-224. https://doi.org/10.1016/j.jclepro.2019.01.324.

[4] A. Yang, W. Shen, S.A. Wei, L. Dong, J. Li, V. Gerbaud, Design and control of pressure-swing distillation for separating ternary systems with three binary minimum azeotropes, AIChE Journal 65(4) (2019) 1281-1293. https://doi.org/10.1002/aic.16526.

[5] J. Qi, Y. Li, J. Xue, R. Qiao, Z. Zhang, Q. Li, Comparison of heterogeneous azeotropic distillation and energy-saving extractive distillation for separating the acetonitrile-water mixtures, Separation and Purification Technology 238 (2020) 116487. https://doi.org/10.1016/j.seppur.2019.116487.

[6] L. Zhao, X. Lyu, W. Wang, J. Shan, T. Qiu, Comparison of heterogeneous azeotropic distillation and extractive distillation methods for ternary azeotrope ethanol/toluene/water separation, Computers & Chemical Engineering 100 (2017) 27-37. https://doi.org/10.1016/j.compchemeng.2017.02.007.

[7] M.A. Santaella, L.E. Jiménez, A. Orjuela, J.G. Segovia-Hernández, Design of thermally coupled reactive distillation schemes for triethyl citrate production using economic and controllability criteria, Chemical Engineering Journal 328 (2017) 368-381. https://doi.org/10.1016/j.cej.2017.07.015.

[8] J. Holtbruegge, S. Heile, P. Lutze, A. Górak, Synthesis of dimethyl carbonate and propylene glycol

in a pilot-scale reactive distillation column: Experimental investigation, modeling and process analysis, Chemical Engineering Journal 234 (2013) 448-463. https://doi.org/10.1016/j.cej.2013.08.054.

[9] G. Guillén-Gosálbez, F. You, Á. Galán-Martín, C. Pozo, I.E. Grossmann, Process systems engineering thinking and tools applied to sustainability problems: current landscape and future opportunities, Current Opinion in Chemical Engineering 26 (2019) 170-179. https://doi.org/10.1016/j.coche.2019.11.002.

[10] A.A. Kiss, R. Smith, Rethinking energy use in distillation processes for a more sustainable chemical industry, Energy 203 (2020). https://doi.org/10.1016/j.energy.2020.117788.

[11] H. Yu, T. Gundersen, X. Feng, Process integration of organic Rankine cycle (ORC) and heat pump for low temperature waste heat recovery, Energy 160 (2018) 330-340. https://doi.org/https://doi.org/10.1016/j.energy.2018.07.028.

[12] M.R. Eden, A. Koggersbol, L. Hallager, S.B. Jorgensen, Dynamics and control during startup of heat integrated distillation column, Computers & Chemical Engineering 24(2-7) (2000) 1091-1097. https://doi.org/10.1016/S0098-1354(00)00488-9.

[13] T. Bisgaard, S. Skogestad, J. Abildskov, J.K.J.C. Huusom, C. Engineering, Optimal operation and stabilising control of the concentric heat-integrated distillation column (HIDiC), 96 (2017) 196-211. https://doi.org/10.1016/j.compchemeng.2016.09.020.

[14] J. Gu, X. You, C. Tao, J. Li, V. Gerbaud, Energy-Saving Reduced-Pressure Extractive Distillation with Heat Integration for Separating the Biazeotropic Ternary Mixture Tetrahydrofuran–Methanol–Water, Industrial & Engineering Chemistry Research 57(40) (2018) 13498-13510. https://doi.org/10.1021/acs.iecr.8b03123.

[15] N. Wang, Q. Ye, L. Chen, H. Zhang, J. Zhong, Improving the economy and energy efficiency of separating water/acetonitrile/isopropanol mixture via triple-column pressure-swing distillation with heat-pump technology, Energy 215 (2021) 119126. https://doi.org/10.1016/j.energy.2020.119126.

[16] X. You, T. Ma, T. Qiu, Design and Optimization of Sustainable Pressure Swing Distillation for Minimum-Boiling Azeotrope Separation, Industrial & Engineering Chemistry Research 58(47) (2019) 21659-21670. https://doi.org/10.1021/acs.iecr.9b04294.

[17] Y. Dai, S. Li, D. Meng, J. Yang, P. Cui, Y. Wang, Z. Zhu, J. Gao, Y. Ma, Economic and Environmental Evaluation for Purification of Diisopropyl Ether and Isopropyl Alcohol via Combining Distillation and Pervaporation Membrane, ACS Sustainable Chemistry & Engineering 7(24) (2019)

20170-20179. https://doi.org/10.1021/acssuschemeng.9b06198.
[18] G.R. Mercado, H. Cabezas, Sustainability in the design, synthesis and analysis of chemical engineering processes, Butterworth-Heinemann2016.
[19] Q. Li, Z. Feng, G.P. Rangaiah, L. Dong, Process Optimization of Heat-Integrated Extractive Dividing-Wall Columns for Energy-Saving Separation of CO2 and Hydrocarbons, Industrial & Engineering Chemistry Research 59(23) (2020) 11000-11011. https://doi.org/10.1021/acs.iecr.0c00666.
[20] World Health Organization, Health in 2015: from MDGs, millennium development goals to SDGs, sustainable development goals.
[21] W.J. Chua, G.P. Rangaiah, K. Hidajat, Design and optimization of isopropanol process based on two alternatives for reactive distillation, Chemical Engineering and Processing: Process Intensification 118 (2017) 108-116. https://doi.org/10.1016/j.cep.2017.04.021.
[22] A. Singh, S. da Cunha, G.P. Rangaiah, Heat-pump assisted distillation versus double-effect distillation for bioethanol recovery followed by pressure swing adsorption for bioethanol dehydration, Separation and Purification Technology 210 (2019) 574-586. https://doi.org/10.1016/j.seppur.2018.08.043.
[23] M. Errico, E. Sanchez-Ramirez, J.J. Quiroz-Ramìrez, B.-G. Rong, J.G. Segovia-Hernandez, Multiobjective Optimal Acetone–Butanol–Ethanol Separation Systems Using Liquid–Liquid Extraction-Assisted Divided Wall Columns, Industrial & Engineering Chemistry Research 56(40) (2017) 11575-11583. https://doi.org/10.1021/acs.iecr.7b03078.
[24] Y. Cui, Z. Zhang, X. Shi, C. Guang, J. Gao, Triple-column side-stream extractive distillation optimization via simulated annealing for the benzene/isopropanol/water separation, Separation and Purification Technology 236 (2020) 116303. https://doi.org/10.1016/j.seppur.2019.116303.
[25] Y. Wu, D. Meng, D. Yao, X. Liu, Y. Xu, Z. Zhu, Y. Wang, J. Gao, Mechanism Analysis, Economic Optimization, and Environmental Assessment of Hybrid Extractive Distillation–Pervaporation Processes for Dehydration of n-Propanol, ACS Sustainable Chemistry & Engineering 8(11) (2020) 4561-4571. https://doi.org/10.1021/acssuschemeng.0c00263.
[26] G. Guillén-Gosálbez, A novel MILP-based objective reduction method for multi-objective optimization: Application to environmental problems, Computers & Chemical Engineering 35(8) (2011) 1469-1477. https://doi.org/10.1016/j.compchemeng.2011.02.001.

[27] L. Zhou, H. Tokos, D. Krajnc, Y. Yang, Sustainability performance evaluation in industry by composite sustainability index, Clean Technologies and Environmental Policy 14(5) (2012) 789-803. https://doi.org/10.1007/s10098-012-0454-9.

[28] Y. Liu, R. Lin, J. Ren, Developing a life cycle composite footprint index for sustainability prioritization of sludge-to-energy alternatives, Journal of Cleaner Production 281 (2021) 124885. https://doi.org/10.1016/j.jclepro.2020.124885.

[29] Z. Zhang, C. Wang, C. Guang, B. Stewart, Cost-saving and control investigation for isopentyl acetate ionic liquid catalyzed synthesis through conventional and dividing-wall reactive distillation, Process Safety and Environmental Protection 129 (2019) 89-102. https://doi.org/10.1016/j.psep.2019.06.021.

[30] Z. Feng, W. Shen, G.P. Rangaiah, L. Dong, Design and control of vapor recompression assisted extractive distillation for separating n-hexane and ethyl acetate, Separation and Purification Technology 240 (2020). https://doi.org/10.1016/j.seppur.2020.116655.

[31] Y. Su, S. Jin, X. Zhang, W. Shen, M.R. Eden, J. Ren, Stakeholder-oriented multi-objective process optimization based on an improved genetic algorithm, Computers & Chemical Engineering 132 (2020). https://doi.org/10.1016/j.compchemeng.2019.106618.

[32] X.L. Yang, J.D. Ward, Extractive distillation optimization using simulated annealing and a process simulation automation server, Industrial & Engineering Chemistry Research 57(32) (2018) 11050-11060. https://doi.org/10.1021/acs.iecr.8b00711.

[33] X. Qian, S. Jia, K. Huang, H. Chen, Y. Yuan, L. Zhang, Optimal design of Kaibel dividing wall columns based on improved particle swarm optimization methods, Journal of Cleaner Production 273 (2020). https://doi.org/10.1016/j.jclepro.2020.123041.

[34] G.P. Rangaiah, Z. Feng, A.F. Hoadley, Multi-Objective Optimization Applications in Chemical Process Engineering: Tutorial and Review, Processes 8(5) (2020). https://doi.org/10.3390/pr8050508.

[35] NOMAD - A blackbox optimization software. https://www.gerad.ca/nomad/.

[36] C. Audet, W. Hare, Derivative-free and blackbox optimization, Springer2017.

[37] Y. Song, Y. Du, R. Wang, H. Yan, F. Luo, L. Sun, Vapor–Liquid Equilibria and Conceptual Design of Extractive Distillation for Separating Ethanol and Ethyl Propionate, Journal of Chemical & Engineering Data 65(7) (2020) 3428-3437. https://doi.org/10.1021/acs.jced.9b01162.

[38] Z. Xing, Y. Gao, H. Ding, X. Wang, L. Li, H. Zhou, Isobaric vapor–liquid equilibrium for ternary

system of ethanol, ethyl propionate and para-xylene at 101.3kPa, Chinese Journal of Chemical Engineering 26(3) (2018) 560-565. https://doi.org/10.1016/j.cjche.2017.10.020.
[39] J. Rezaei, Best-worst multi-criteria decision-making method, Omega 53 (2015) 49-57. https://doi.org/10.1016/j.omega.2014.11.009.
[40] J.-J. Wang, Y.-Y. Jing, C.-F. Zhang, J.-H. Zhao, Review on multi-criteria decision analysis aid in sustainable energy decision-making, Renewable and Sustainable Energy Reviews 13(9) (2009) 2263-2278. https://doi.org/10.1016/j.rser.2009.06.021.
[41] A. Kumar, B. Sah, A.R. Singh, Y. Deng, X. He, P. Kumar, R.C. Bansal, A review of multi criteria decision making (MCDM) towards sustainable renewable energy development, Renewable and Sustainable Energy Reviews 69 (2017) 596-609. https://doi.org/10.1016/j.rser.2016.11.191.
[42] M. Brunelli, Introduction to the analytic hierarchy process, Springer2014.
[43] R.A. Horn, C.R. Johnson, Matrix analysis, Cambridge university press2012.
[44] S. Bozóki, Solution of the least squares method problem of pairwise comparison matrices, Central European Journal of Operations Research 16(4) (2008) 345. https://doi.org/10.1007/s10100-008-0063-1.
[45] Y. Liu, J. Ren, Y. Man, R. Lin, C.K.M. Lee, P. Ji, Prioritization of sludge-to-energy technologies under multi-data condition based on multi-criteria decision-making analysis, Journal of Cleaner Production 273 (2020) 123082. https://doi.org/10.1016/j.jclepro.2020.123082.
[46] P.J. Van Laarhoven, W.J.F.s. Pedrycz, Systems, A fuzzy extension of Saaty's priority theory, Fuzzy sets and systems 11(1-3) (1983) 229-241. https://doi.org/10.1016/S0165-0114(83)80082-7.
[47] Y.M. Wang, T.M. Elhag, Z. Hua, A modified fuzzy logarithmic least squares method for fuzzy analytic hierarchy process, Fuzzy sets and systems 157(23) (2006) 3055-3071. https://doi.org/10.1016/j.fss.2006.08.010.
[48] S. Guo, H. Zhao, Fuzzy best-worst multi-criteria decision-making method and its applications, Knowlede-based systems 121 (2017) 23-31. https://doi.org/10.1016/j.knosys.2017.01.010.
[49] C. Audet, J.E. Dennis Jr, Mesh adaptive direct search algorithms for constrained optimization, SIAM Journal on optimization 17(1) (2006) 188-217. https://doi.org/doi.org/10.1137/040603371.
[50] S.L. Digabel, Algorithm 909: NOMAD: Nonlinear Optimization with the MADS Algorithm, ACM Trans. Math. Softw. 37(4) (2011) Article 44. https://doi.org/10.1145/1916461.1916468.
[51] Andrés F. Abril (2021). Aspen Plus - Matlab Link

(https://www.mathworks.com/matlabcentral/fileexchange/69464-aspen-plus-matlab-link), MATLAB Central File Exchange. Retrieved May 27, 2021.

[52] V. Pleşu, A.E. Bonet Ruiz, J. Bonet, J. Llorens, Simple Equation for Suitability of Heat Pump Use in Distillation, 24th European Symposium on Computer Aided Process Engineering2014, pp. 1327-1332. https://doi.org/10.1016/b978-0-444-63455-9.50056-8.

[53] Q. Zhang, M. Liu, A. Zeng, Performance enhancement of pressure-swing distillation process by the combined use of vapor recompression and thermal integration, Computers & Chemical Engineering 120 (2019) 30-45. https://doi.org/10.1016/j.compchemeng.2018.09.014.

[54] A. Yang, S. Jin, W. Shen, P. Cui, I.L. Chien, J. Ren, Investigation of energy-saving azeotropic dividing wall column to achieve cleaner production via heat exchanger network and heat pump technique, Journal of Cleaner Production (2019). https://doi.org/10.1016/j.jclepro.2019.06.224.

[55] S.K. Sikdar, Sustainable development and sustainability metrics, 49(8) (2003) 1928-1932.

[56] X. Zhao, F. You, Sustainable Process Design and Synthesis for HDPE Recycling, Computer Aided Chemical Engineering 50 (2021) 31-36. https://doi.org/10.1016/B978-0-323-88506-5.50006-1.

[57] A. Carvalho, R. Gani, H. Matos, Design of sustainable chemical processes: Systematic retrofit analysis generation and evaluation of alternatives, Process Safety and Environmental Protection 86(B5) (2008) 328-346. https://doi.org/10.1016/j.psep.2007.11.003.

[58] A. Agarwal, D. Sengupta, M. El-Halwagi, Sustainable Process Design Approach for On-Purpose Propylene Production and Intensification, ACS Sustainable Chemistry & Engineering 6(2) (2018) 2407-2421. https://doi.org/10.1021/acssuschemeng.7b03854.

[59] A. Yang, Y. Su, L. Teng, S. Jin, T. Zhou, W. Shen, Investigation of energy-efficient and sustainable reactive/pressure-swing distillation processes to recover tetrahydrofuran and ethanol from the industrial effluent, Separation and Purification Technology 250 (2020). https://doi.org/10.1016/j.seppur.2020.117210.

[60] Ž. Olujić, L. Sun, A. de Rijke, P.J. Jansens, Conceptual design of an internally heat integrated propylene-propane splitter, Energy 31(15) (2006) 3083-3096. https://doi.org/10.1016/j.energy.2006.03.030.

[61] Z. Feng, W. Shen, G.P. Rangaiah, L. Lv, L. Dong, Process Development, Assessment, and Control of Reactive Dividing-Wall Column with Vapor Recompression for Producing n-Propyl Acetate, Industrial & Engineering Chemistry Research 58(1) (2018) 276-295.

https://doi.org/10.1021/acs.iecr.8b05122.
[62] W.L. Luyben, Distillation Design and Control Using Aspen™ Simulation, John Wiley & Sons2013.
[63] Q. Yang, S. Zhu, Q. Yang, W. Huang, P. Yu, D. Zhang, Z. Wang, Comparative techno-economic analysis of oil-based and coal-based ethylene glycol processes, Energy Conversion and Management 198 (2019) 111814. https://doi.org/10.1016/j.enconman.2019.111814.
[64] MOLBASE http://jiage.molbase.cn/.
[65] M.A. Gadalla, Z. Olujic, P.J. Jansens, M. Jobson, R. Smith, Reducing CO2 Emissions and Energy Consumption of Heat-Integrated Distillation Systems, Environmental Science & Technology 39(17) (2005) 6860-6870. https://doi.org/10.1021/es049795q.
[66] X. Li, Y. Zhang, L. Fang, Z. Jin, Y. Zhang, X. Yu, X. Ma, N. Deng, Z. Wu, Energy, exergy, economic, and environmental analysis of an integrated system of high-temperature heat pump and gas separation unit, Energy Conversion and Management 198 (2019). https://doi.org/10.1016/j.enconman.2019.111911.
[67] B. Dai, H. Qi, S. Liu, Z. Zhong, H. Li, M. Song, M. Ma, Z. Sun, Environmental and economical analyses of transcritical CO2 heat pump combined with direct dedicated mechanical subcooling (DMS) for space heating in China, Energy Conversion and Management 198 (2019). https://doi.org/10.1016/j.enconman.2019.01.119.
[68] F.I. Khan, S.A. Abbasi, Multivariate hazard identification and ranking system, Process Safety Progress 17(3) (1998) 157-170. https://doi.org/10.1002/prs.680170303.
[69] A. Castillo-Landero, A.P. Ortiz-Espinoza, A. Jiménez-Gutiérrez, A Process Intensification Methodology Including Economic, Sustainability, and Safety Considerations, Industrial & Engineering Chemistry Research 58(15) (2019) 6080-6092. https://doi.org/10.1021/acs.iecr.8b04146.
[70] J.D. Seader, E.J. Henley, D.K. Roper, Separation process principles Wiley New York1998.
[71] S. Sun, L. Lü, A. Yang, S.a. Wei, W. Shen, Extractive distillation: Advances in conceptual design, solvent selection, and separation strategies, Chinese Journal of Chemical Engineering 27(6) (2019) 1247-1256. https://doi.org/10.1016/j.cjche.2018.08.018.
[72] V. Gerbaud, I. Rodriguez-Donis, L. Hegely, P. Lang, F. Denes, X. You, Review of extractive distillation. Process design, operation, optimization and control, Chemical Engineering Research and Design 141 (2019) 229-271. https://doi.org/10.1016/j.cherd.2018.09.020.

[73] V. Kiva, E. Hilmen, S. Skogestad, Azeotropic phase equilibrium diagrams: a survey, Chemical engineering science 58(10) (2003) 1903-1953. https://doi.org/10.1016/S0009-2509(03)00018-6.

[74] S. Tututi-Avila, N. Medina-Herrera, J. Hahn, A. Jiménez-Gutiérrez, Design of an energy-efficient side-stream extractive distillation system, Computers & Chemical Engineering 102 (2017) 17-25. https://doi.org/10.1016/j.compchemeng.2016.12.001.

[75] T. Shi, W. Chun, A. Yang, Y. Su, S. Jin, J. Ren, W. Shen, Optimization and control of energy saving side-stream extractive distillation with heat integration for separating ethyl acetate-ethanol azeotrope, Chemical Engineering Science 215 (2019) 115373. https://doi.org/10.1016/j.ces.2019.115373.

[76] A. Yang, Y. Su, I.L. Chien, S. Jin, C. Yan, S.a. Wei, W. Shen, Investigation of an energy-saving double-thermally coupled extractive distillation for separating ternary system benzene/toluene/cyclohexane, Energy (2019). https://doi.org/10.1016/j.energy.2019.07.086.

[77] Y. Zhao, K. Ma, W. Bai, D. Du, Z. Zhu, Y. Wang, J. Gao, Energy-saving thermally coupled ternary extractive distillation process by combining with mixed entrainer for separating ternary mixture containing bioethanol, Energy 148 (2018) 296-308. https://doi.org/10.1016/j.energy.2018.01.161.